JARO (2022)
DOI: 10.1007/s10162-022-00858-y

JARO
Journal of the Association for Research in Otolaryngology

Research Article

Insights into Inner Ear Function and Disease Through Novel Visualization of the Ductus Reuniens, a Seminal Communication Between Hearing and Balance Mechanisms

Christopher M. Smith[1,2,3], Ian S. Curthoys[4], Stefan K. Plontke[5], Matthias Menzel[6], Payal Mukherjee[7], Christopher Wong[4], and Jeffrey T. Laitman[1,2,3,8]

[1] *Center for Anatomy and Functional Morphology, Icahn School of Medicine at Mount Sinai, Annenberg Building Room 12-90, 1468 Madison Ave, New York, NY 10029, USA*

[2] *Department of Anthropology, The Graduate Center, City University of New York, New York, NY, USA*

[3] *New York Consortium in Evolutionary Primatology, New York, NY, USA*

[4] *Vestibular Research Laboratory, School of Psychology, University of Sydney, Sydney, NSW, Australia*

[5] *Department of Otorhinolaryngology, Head and Neck Surgery, Martin Luther University Halle-Wittenberg, Halle (Saale), Germany*

[6] *Fraunhofer Institute for Microstructure of Materials and Systems, Halle (Saale), Germany*

[7] *RPA Institute of Academic Surgery, Royal Prince Alfred Hospital, Sydney, NSW, Australia*

[8] *Department of Otolaryngology, Icahn School of Medicine at Mount Sinai, New York, NY, USA*

Received: 28 January 2022; accepted: 29 June 2022

ABSTRACT

The sensory end-organs responsible for hearing and balance in the mammalian inner ear are connected via a small membranous duct known as the ductus reuniens (also known as the reuniting duct (DR)). The DR serves as a vital nexus linking the hearing and balance systems by providing the only endolymphatic connection between the cochlea and vestibular labyrinth. Recent studies have hypothesized new roles of the DR in inner ear function and disease, but a lack of knowledge regarding its 3D morphology and spatial configuration precludes testing of such hypotheses. We reconstructed the 3D morphology of the DR and surrounding anatomy using osmium tetroxide micro-computed tomography and digital visualizations of three human inner ear specimens. This provides a detailed, quantitative description of the DR's morphology, spatial relationships to surrounding structures, and an estimation of its orientation relative to head position. Univariate measurements of the DR, inner ear, and cranial planes were taken using the software packages 3D Slicer and Zbrush. The DR forms a narrow, curved, flattened tube varying in lumen size, shape, and wall thickness, with its middle third being the narrowest. The DR runs in a shallow bony sulcus superior to the osseus spiral lamina and adjacent to a ridge of bone that we term the "crista reuniens" oriented posteromedially within the cranium. The DR's morphology and structural configuration relative to surrounding anatomy has important implications for understanding aspects of inner ear function and disease, particularly after surgical alteration of the labyrinth and potential causative factors for Ménière's disease.

Keywords: Vestibular system, Membranous labyrinth, Inner ear, Ductus reuniens, Otolith organs, Cochlea

Correspondence to: Christopher M. Smith · · Center for Anatomy and Functional Morphology, Icahn School of Medicine at Mount Sinai · Annenberg Building Room 12-90, 1468 Madison Ave, New York, NY, 10029, USA. email: Christopher.smith1@mssm.edu

INTRODUCTION

The mammalian inner ear contains the sensory end-organs for hearing (cochlea) and balance (peripheral vestibular system) housed within the petrosal region of the temporal bone. These end-organs comprise the membranous labyrinth (containing endolymph) encased within a bony otic capsule (often referred to as the bony labyrinth). Of the structures that make up the membranous labyrinth, the ductus reuniens (DR) remains one of the most poorly understood in terms of its morphology and spatial relationships to surrounding structures. The DR forms the only endolymphatic connection between the auditory and vestibular end organs of the ear joining the inferior portion of the saccule (of the vestibular labyrinth) to the cochlear duct (also called scala media of the cochlea containing additional non-endolymphatic spaces, e.g., the space of Nuel). Examining the morphology of this connection is vital to clearly understand the form and function of the peripheral auditory and vestibular systems. In particular, elucidating DR morphology and spatial configuration will contribute to both clinical and evolutionary studies of the inner ear. Indeed, previous work suggests the importance of the DR in protecting vestibular function during surgical trauma to the cochlea (see Plontke et al. 2021). This, and other hypotheses, can be tested further with a comprehensive understanding of DR structure.

This study provides the first comprehensive description of the 3D morphology of the human DR, its relationship to surrounding anatomy (e.g., stapes footplate and round window) and orientation relative to head position using osmium tetroxide microcomputed tomography (μCT) and digital visualizations. We chose this approach as 3D spatial relationships of hard and soft tissue cannot be determined using only histological, 2D imaging and/or traditional μCT techniques. By improved visualization of the DR, we will achieve a new understanding of morphological relationships between the DR and other structures within the inner ear and cranium.

Our results visualize the DR as a thin, subtly curved hourglass-shaped duct running along a ridge of bone which we term the "crista reuniens" (CR) adjacent to the round window. The duct can be divided into thirds, with a "vestibular third", a "middle third" and "cochlear third" each varying in characteristics of lumen shape, lumen width, and/or wall thickness. The patency of this duct also seems to vary as there are several points within the middle third where the lumen could not be discerned. These findings have important implications for the following: (1) testing hypotheses as to the protective function of the DR in preserving vestibular function during surgeries involving cochlear removal; (2) the potential role of the DR in Ménière's disease; and (3) studies into the evolution of auditory and vestibular end-organ structure and communication.

MATERIALS AND METHODS

Data Acquisition and Reconstruction

Our sample is divided into two groups: (1) three individual human otic capsules used to visualize the DR; (2) nine adult human dry crania used to visualize the orientation of the CR relative to head position.

Group 1: Otic Capsules

Our initial sample consisted of 13 otic capsules derived from μCT of specimens stained by osmium tetroxide (Uzun et al. 2007). Of these, only three were found to have a clear representation of the DR. The size of our sample reflects the challenges of staining and imaging, and difficulty in obtaining views of the DR. Initial surgical preparation of the temporal bones was conducted by PM, ISC oversaw all steps and did the staining, and CW carried out the μCT scans. μCT shows membranous and bony structures at high resolution and was therefore chosen to examine the DR in this case (Mukherjee et al. 2011, 2019).

Procedures on human temporal bones were approved by the NSW Department of Health and by the Royal Prince Alfred Hospital Ethics Office (protocol number X19-0480). For the fusion images in Fig. 8, a formaldehyde-preserved human temporal bone from a body donor was used. The procedure was in accordance with the ethical standards of the responsible committee (Ethics Committee of the Martin Luther University Halle-Wittenberg, Germany, approval number: 2020–176).

Three cadaveric temporal bones were drilled to isolate the otic capsule. All temporal bones were fixed in Karnovsky's fixative (3% paraformaldehyde, 0.5% glutaraldehyde in phosphate buffer) for 24 h. This method is known to minimize shrinkage (Anniko and Lundquist 1977). The temporal bones were then soaked in 2 per cent osmium tetroxide, for up to 9 days, and scanned in a 64-bit μCT scanner (MicroXCT-400; Xradia, Pleasanton, California, USA). Scan width ranged from 9.4 to 11 μm. The μCT data were saved in tagged image file format (.TIFF) files and were cropped to focus on the labyrinth. Detailed scanning parameters have been described in earlier publications (Mukherjee et al. 2019; Uzun et al. 2007; Uzun-Coruhlu et al. 2007).

The stained μCT stack of.TIFF images were imported into the software 3D Slicer, version 4.10.1 (3D Slicer 2020; Fedorov et al. 2012; Kikinis et al. 2014), following Smith et al. (2021) enabling 3D reconstruction. The membranous labyrinth was reconstructed along with the bony labyrinth, utricular macula, saccular macula, stapes, and round window. Each bony labyrinth was segmented

using semi-automated thresholding to define the boundary between the fluid-filled spaces of the labyrinth and surrounding bone. Automatic segmentation in the osmium tetroxide μCT.TIFF stack proved inadequate to discern the DR in its entirety. Therefore, the membranous labyrinth and maculae were manually segmented using the "draw" tool in 3D Slicer. Segmentations were exported as.OBJ files and imported into the software Zbrush (v. 2021.6.6; Pixologic 2020) where the surface topology was smoothed, and artifacts removed in surface meshes.

Upon initial observations, the DR appears to vary in lumenal size and shape. To get as robust a visualization as possible, we divided the DR into three equidistant regions a priori: a vestibular, middle, and cochlear third. Each region spans ~ 0.37 mm.

Group 2: Dry Crania

The nine dry crania were obtained from the collections of the American Museum of Natural History (AMNH), Division of Anthropology and scanned using a GE Phoenix Vtome Xs μCT scanner housed within the AMNH Microscopy Imaging Facility. Scan width ranged from 83 to 110 μm. Each μCT stack was exported as a series of.DICOM images and then imported into the software 3D Slicer for automatic segmentation of the cranium and semi-automatic segmentation of each bony labyrinth.

Data Analysis

Three sets of measures were taken: (1) measurements of the DR on μCT slices in 3D Slicer; (2) measurements of the DR on 3D reconstructions in Zbrush; and (3) measurements of the CR and cranium in 3D Slicer, for a total of nine measures. The first two sets used the group 1 sample. The third set used the group 2 sample.

Group 1: DR Measurements on μCT Slices in 3D Slicer

1. Length of DR (measured from the point of superoinferior expansion of the DR joining the saccule (vestibular end) to the point of superoinferior expansion joining the cochlear duct (cochlear end); see Fig. 1A).
2. Intralumenal width at vestibular end.
3. Intralumenal width at cochlear end.
4. Minimum intralumenal width of the DR (see Fig. 1B).
5. Thickness of DR wall at three points along the length of the duct (vestibular end, point of minimum intralumenal width, and cochlear end). Each thickness measure was averaged from three measures of wall thickness at the superior, anterior, and posterior borders of the DR. The inferior wall thickness could not be discerned due to poor visibility of the wall abutting the bone.

Group 1: DR Measurements on 3D Reconstructions in Zbrush

6. Minimum distance of DR from stapes footplate (measured from posteroinferior edge of stapes footplate to anterolateral end of DR).
7. Minimum distance of DR from superiormost point on posteromedial corner of round window membrane.

Group 2: CR Measurements on 3D Reconstructions in 3D Slicer

8. Angle between planes fit to the orientations of the CR and midsagittal plane (MSP). MSP was constructed from three craniometric landmarks (nasion, acanthion, and opisthion). These points were chosen to account for the plane that best fit external landmarks of the cranium spanning the upper face, lower face and posterior basicranium. All angle measures are taken medially (i.e., the angle formed towards midline) (Fig. 2A).

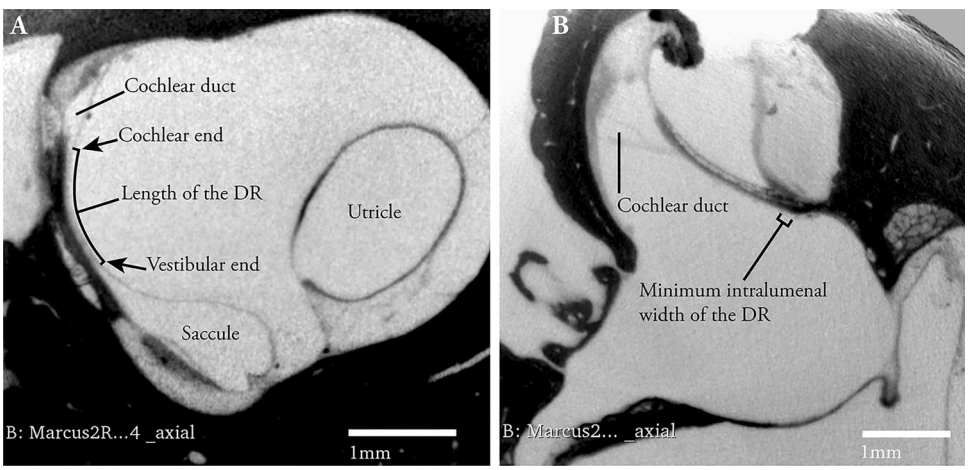

Fig. 1 Images from μCT scans of the inner ear labyrinth stained with osmium tetroxide. **A** View along DR length. **B** Cross-sectional view of middle third of DR

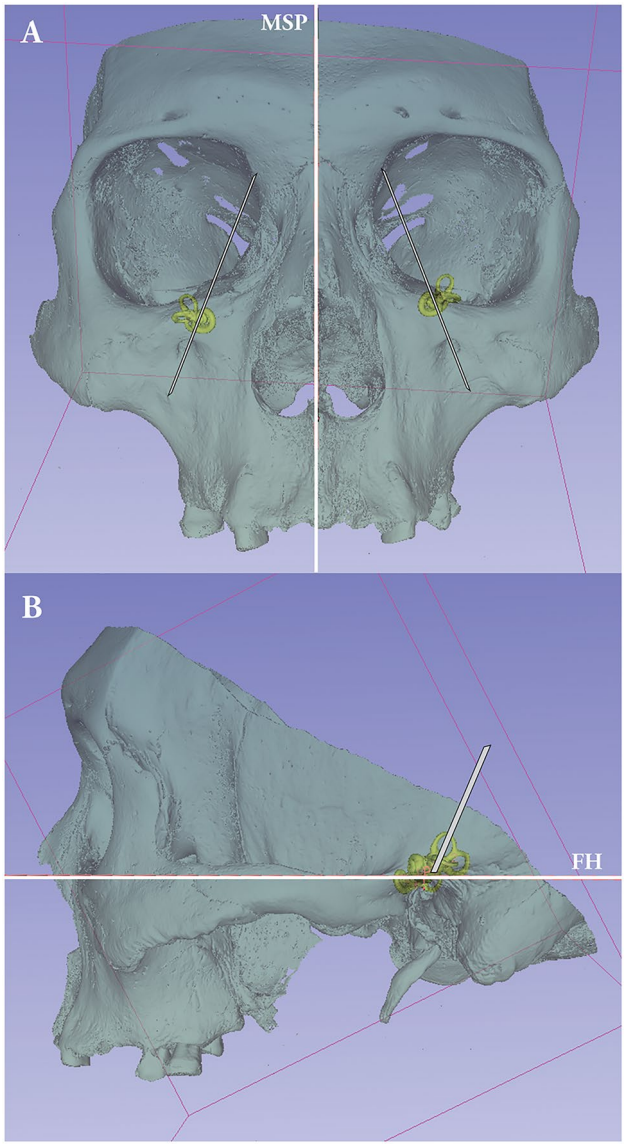

Fig. 2 Screenshots from 3D slicer showing planes of orientation. Cranial planes (**A** constructed from MSP, **B** constructed from FH) shown as solid white lines. Planes measuring CR orientation shown as transparent white planes with black outlines

9. Angle between planes fit to the orientation of the CR and a plane formed from Frankfurt horizontal (FH) (Fig. 2B).

RESULTS

Anatomical Description

Overall, the DR forms a narrow, slightly flattened tube which has a subtle hourglass-like shape. The vestibular and cochlear thirds expand slightly at the junction with the saccule and cochlear duct, respectively. The DR is curved concavely when viewed anteroposteriorly, adhering to the inferior bony wall of the vestibule anterior to the posterior ampulla and superior to the bony arch of the round window (Figs. 3 and 4A–C).

As the DR runs along the bony wall, it travels within a shallow bony sulcus and abuts a ridge of bone (the CR). The CR runs posterior to the osseus spiral lamina (OSL) from which it may be structurally related due to continuity observed between the two. The CR is observable on both the internal and external morphology of the bony wall of the labyrinth (Fig. 5A, B). and spans, externally, from the posteriormost point of the spherical recess to the posteromedial corner of round window (Fig. 5B). The posterior vestibular artery and vein run superficial to this crista.

Measurements (Group 1)

Metric results are as follows (see also Tables 1, 2 and 3):

1. Average length of the DR: *1.09 mm* (± 0.076 mm; range = 1.00–1.14 mm).
2. Average intralumenal width at vestibular end: *0.407 mm* (± 0.031 mm; range = 0.373–0.428 mm).
3. Average intralumenal width at cochlear end: *0.439 mm* (± 0.058 mm; range = 0.381–0.496 mm).
4. Average minimum intralumenal width: *0.142 mm* (± 0.007 mm; range = 0.139–0.145 mm).
5. Thickness of DR wall at vestibular end: *0.039 mm* (± 0.017 mm); point of minimum intralumenal width: *0.027 mm* (± 0.011 mm); and cochlear end: *0.026 mm* (± 0.012 mm).
6. Average minimum distance from stapes footplate: *2.07 mm* (± 0.051 mm; range = 2.02–2.12 mm).
7. Average minimum distance from superiormost point on posteromedial corner of round window membrane: *0.25 mm* (± 0.006 mm; range = 0.25–0.26 mm).

The thinnest intralumenal width occurs in the middle and cochlear thirds of each DR. The degree to which the vestibular and cochlear ends expand out from this narrow middle third varies across individuals (Fig. 6).

In all three specimens the DR was patent throughout most of its trajectory, but in two specimens several slices showed a flattening of the duct itself occurring in the middle third. Intralumenal measurements were only taken on slices where the lumen could be discerned.

Characteristics of DR Regions

Our metrical analyses reveal characteristics of the three DR regions (vestibular, middle, and cochlear thirds). The vestibular third has the thickest walls of the DR and joins it to the inferior portion of the saccule. The middle third is characterized by the narrowest intralumenal width ($\bar{X}$ = 0.14 mm) and comprises the slender portion of

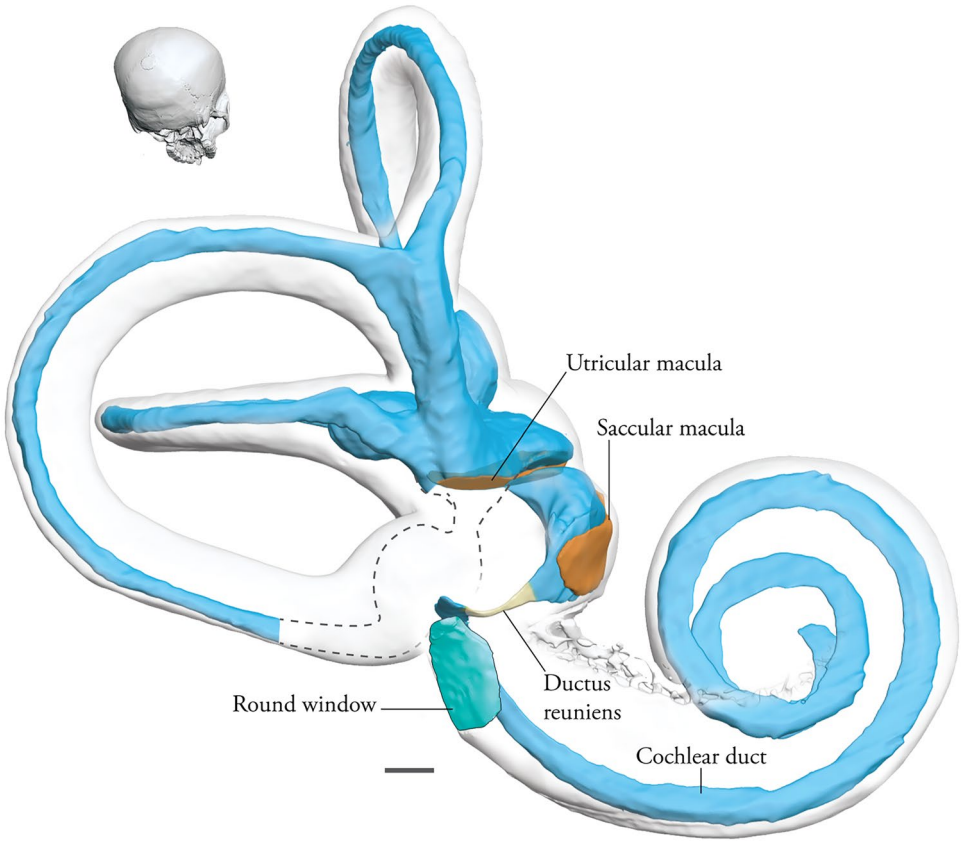

Fig. 3 3D reconstruction of the left membranous labyrinth (blue; minus the saccular, utriculoendolymphatic, and endolymphatic ducts) shown in posterior oblique view. The bony labyrinth is transparent. The posterior ampulla (dotted line) is removed to visualize DR (yellow). Maculae are shown in orange and round window in turquoise. Cranium shows orientation of the head. Scale bar is 1 mm

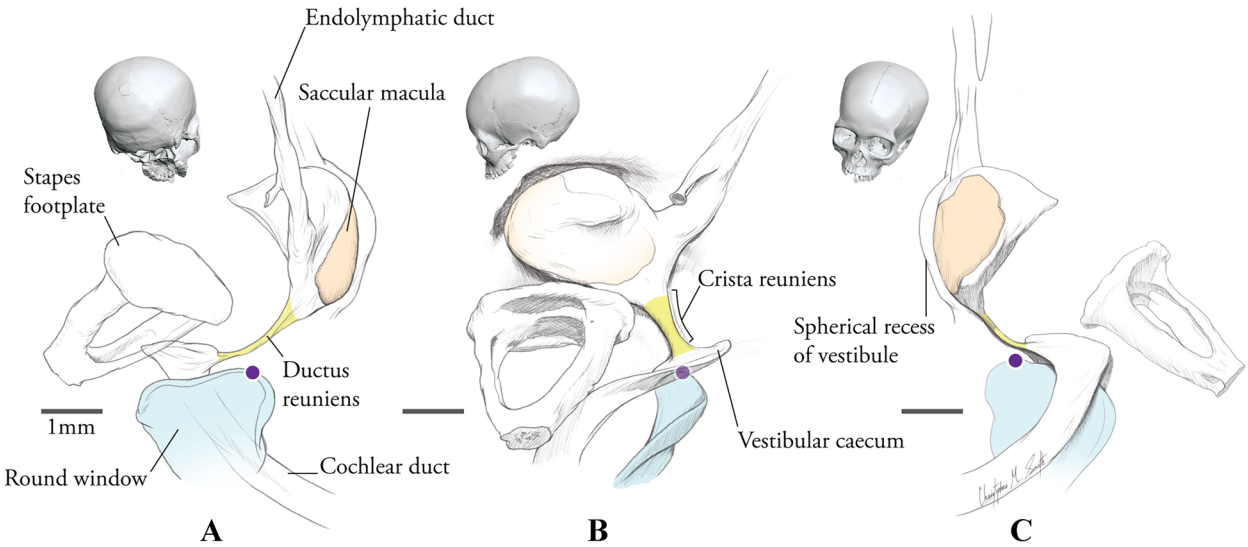

Fig. 4 Illustration of the left DR in three views. **A** Posterolateral view. **B** Superolateral view. **C** Anterosuperior view. Purple dot signifies superiormost point on posteromedial corner of round window. Crania show orientation of the head for each view. Scale bars are 1 mm

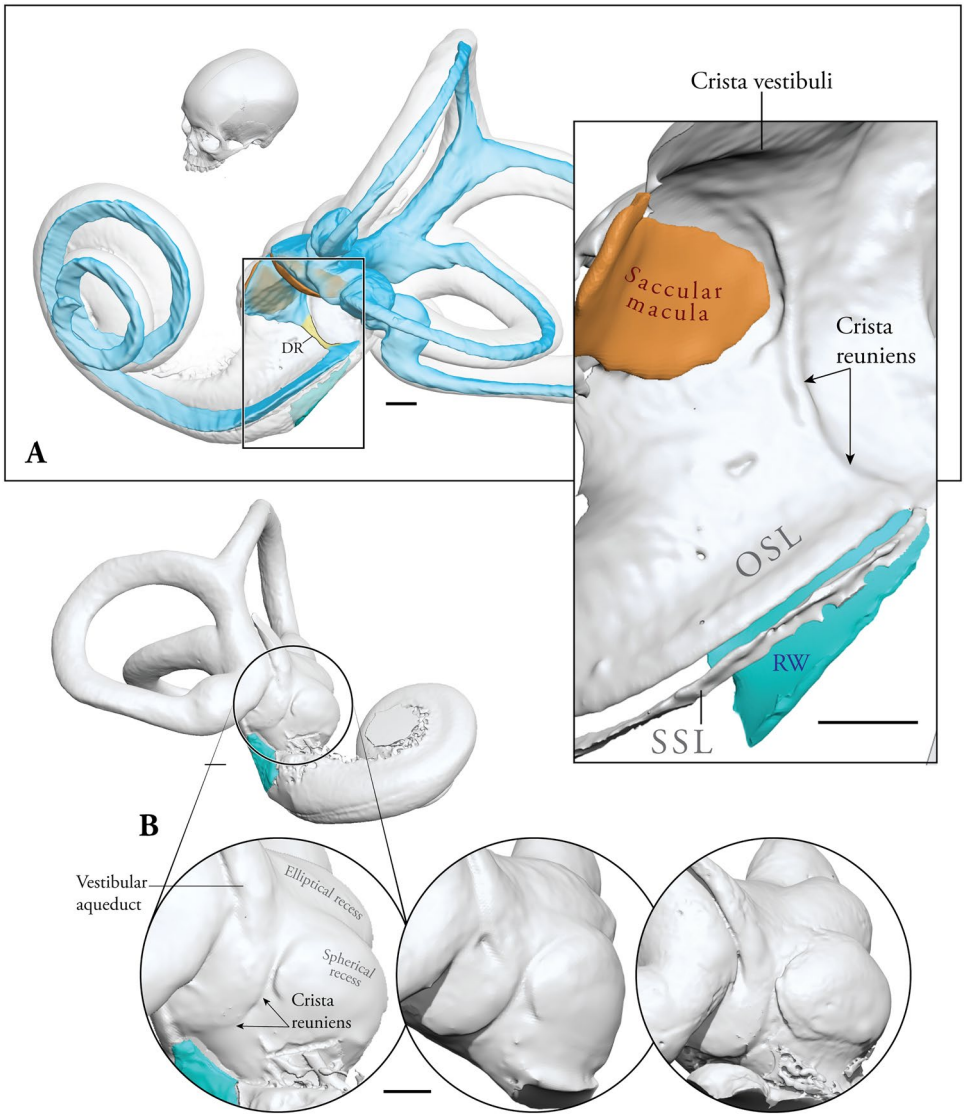

Fig. 5 The DR in relation to the crista reuniens shown on 3D reconstructions. **A** The left membranous labyrinth showing the DR against bony wall; inset shows the crista reuniens with otic labyrinth (including DR) removed. Cranium shows head orientation. **B** Views of the left crista reuniens in inferomedial view from three individuals. The posterior artery and vein have been removed for visual clarity. OSL, osseus spiral lamina; SSL, secondary spiral lamina. Scale bars are 1 mm

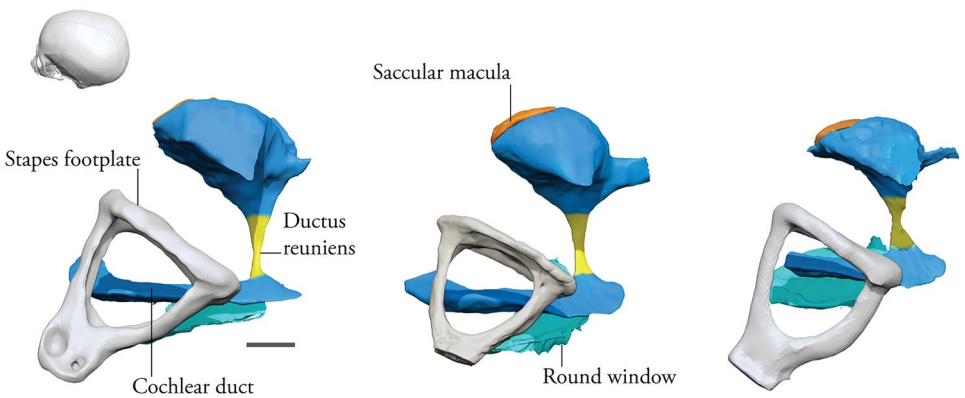

Fig. 6 Comparison of 3D reconstructions of the DR in the group 1 sample. Cranium shows head orientation. Scale bar is 1 mm

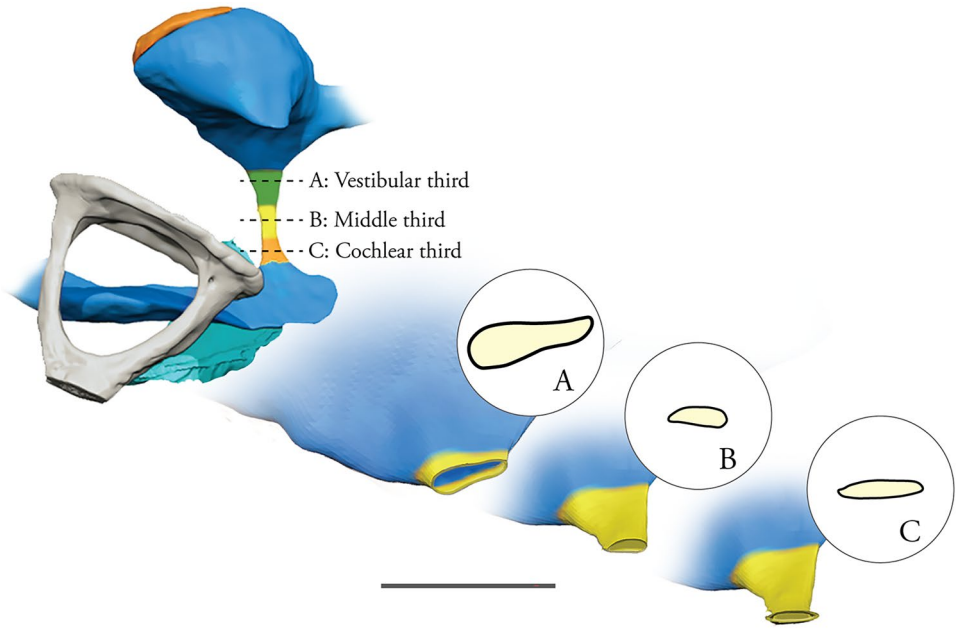

Fig. 7 Regions of the left DR and differences in lumen shape. In the top left image, the vestibular third is highlighted in green; cochlear third is highlighted in orange. **A** Vestibular third cross-section. **B** Middle third cross-section. **C** Cochlear third cross section. Scale bar is 1 mm

TABLE 1

DR metrics taken on μCT slices in 3D Slicer (mm); measurements 1–4

Measurements	*Individual 1*	*Individual 2*	*Individual 3*	$\bar{x}$	*SD*
Length of DR (1)	1.118	1.002	1.144	1.088	0.076
Intralumenal width at vestibular end (2)	0.425	0.373	0.428	0.407	0.031
Intralumenal width at cochlear end (3)	0.441	0.381	0.496	0.439	0.058
Minimum intralumenal width of the DR (4)	0.139	0.145	0.143	0.142	0.007

See "Materials and Methods" section for a description of distances
$\bar{x}$ sample mean, *SD* standard deviation

TABLE 2

DR wall thickness measured on μCT slices in 3D Slicer (mm); measurement 5

Individual	*Vestibular third*	*Middle third*	*Cochlear third*	*Individual mean*	*SD*
1	0.019	0.014	0.014	0.016	0.003
2	0.049	0.034	0.026	0.036	0.012
3	0.048	0.032	0.038	0.039	0.009
$\bar{x}$	0.039	0.027	0.026		
SD	0.017	0.011	0.012		

TABLE 3

DR metrics taken on 3D reconstructions in Zbrush (mm); measurements 6 and 7

Measurements	*Individual 1*	*Individual 2*	*Individual 3*	*X̄*	*SD*
Minimum distance of DR from stapes footplate (6)	2.079	2.018	2.120	2.070	0.051
Minimum distance of DR from round window membrane (7)	0.258	0.246	0.251	0.252	0.006

the DR's hourglass shape. This region is bordered medially and laterally by the vestibular and cochlear thirds, respectively, where they each begin to expand anteroposteriorly from the slender middle third. The cochlear third has similar wall thickness to the middle third and joins the DR to the medial cochlear duct just anterior to the vestibular caecum. The shape of the lumen varies throughout each region (Fig. 7A–C).

Orientation Within the Cranium (Group 2)

The CR is oriented medially when viewed anteroposteriorly (ranging from 31 to 49°) and posteriorly when viewed laterally (ranging from 54 to 79°) (Table 4; Fig. 2). This measure gives an estimation of the orientation of the DR within the cranium as it runs alongside the CR. No significant differences among provenances or between sexes were observed.

DISCUSSION

The DR is a delicate membranous structure providing the only endolymphatic connection between the auditory and vestibular end-organs of the inner ear. Its diminutive size and slight structure have precluded a detailed 3D morphological description, although previous μCT and synchrotron radiation phase-contrast imaging have shown that the DR runs approximately 1.2 mm along its length (Li et al. 2021a, b). Our results show the DR as a curved and slightly flattened tube expanding at both ends to join the saccule and cochlear duct with a narrow and thinly walled middle third. The DR runs superiorly to the OSL, within a shallow bony sulcus and alongside a ridge of bone we term the "crista reuniens" (CR) (oriented posteromedially within the cranium; see Fig. 2). The bony sulcus was initially observed by Yamane et al. (termed the YT groove; 2009) in CT images and cadaveric dissection. The DR is adjacent to the round window, which proves particularly important during surgical approaches to the inner ear (e.g., cochleostomy or round window approaches though a posterior tympantomy or transmeatally; 3D spatial orientation of the DR in these views is shown in Fig. 8A, B).

These results, particularly the identification of a narrow, thinly walled middle third of the DR, have important implications for understanding vestibular function, pathology, and evolution. Most importantly, these include (1) the DR's potential protective role in preserving vestibular function during (surgical) trauma to the cochlea, (2) its possible role in Ménière's disease, and (3) the evolution of the DR and cochlear duct.

TABLE 4

Orientations of crista reuniens (CR) relative to FH and MSP. Sample derived from the AMNH collections; measurements 8 and 9

ID	*Sex*	*Provenance*	*Voxel resolution (mm)*	*Angle b/w left CR and FH*	*Angle b/w right CR and FH*	*Angle b/w left CR and MSP*	*Angle b/w right CR and MSP*
99/101	f	Fort Rupert, BC	0.107	55.7	54.12	45.5	44.4
99/103	m	Fort Rupert, BC	0.100	67.75	70.641	42.979	36.093
99/1716	m	Fort Rupert, BC	0.089	66.17	72.8	31.73	33.5
99/1717	m	Fort Rupert, BC	0.094	75.74	75.17	35.17	44.58
99/1719	m	Fort Rupert, BC	0.089	65.43	65.75	42.5	44
99/1723	m	Fort Rupert, BC	0.101	66.47	69.8	36.2	44
99/1752	f	Eburne, BC	0.101	66.67	66.23	44.63	33.89
99/1800	m	Eburne, BC	0.097	76.2	78.92	48.51	47.21
99.1/127	m	Sonora, MX	0.095	60.07	54.866	58.6	56.75

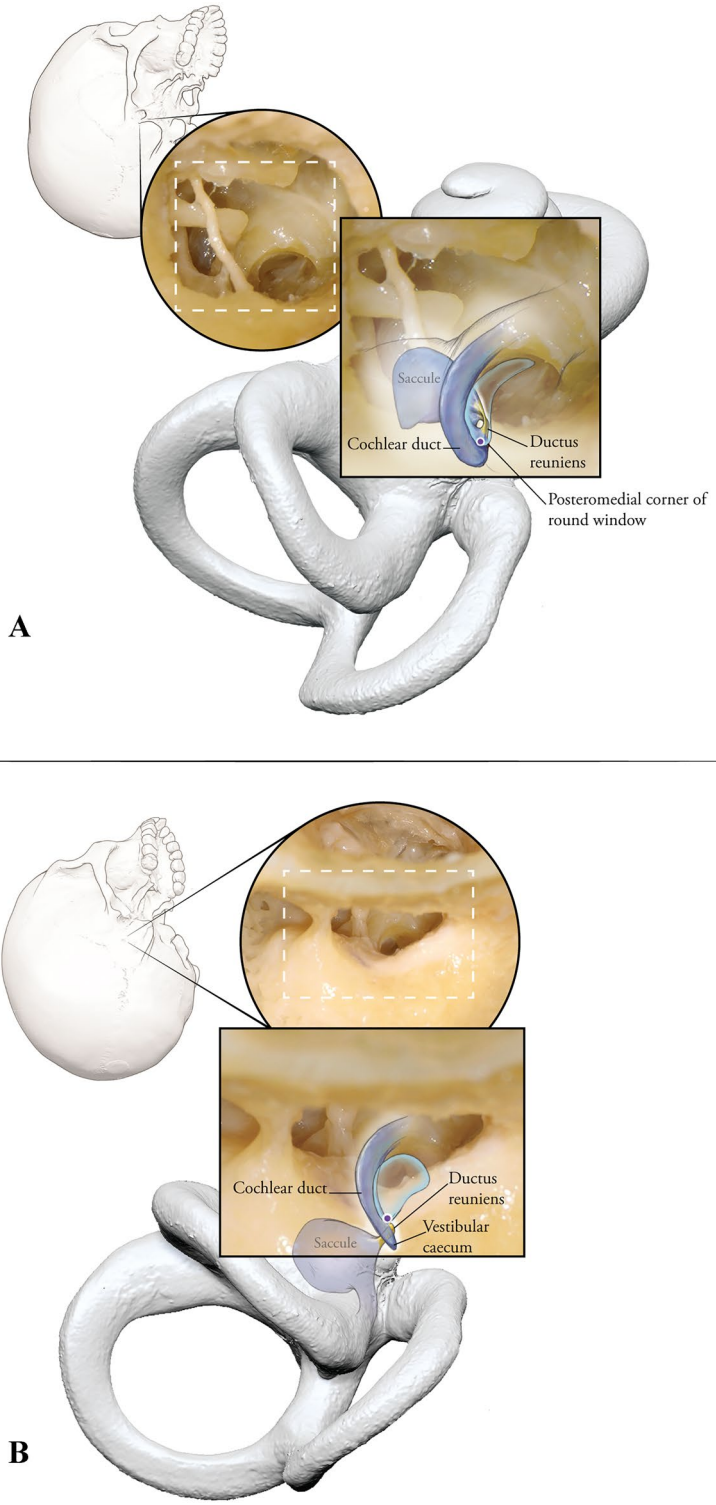

Fig. 8 Views of the right DR in two surgical approaches to the inner ear. 3D reconstructions of the bony labyrinth and DR are overlaid on intraoperative photos of the same individual. **A** Transmeatal approach. **B** Posterior tympanotomy. Purple dot shows superiormost point on posteromedial corner of round window. Crania indicate orientation of the head in each viewpoint.

Preservation of Vestibular Function During Surgery

Previous work has noted that vestibular function can be preserved after partial or subtotal removal of the cochlea in a large case series (Plontke et al. 2021). Preservation of vestibular function could be explained by the anatomical structure of the membranous labyrinth itself and DR morphology as revealed in our study. Several of these features of the membranous labyrinth include a more thickly walled pars superior compared to the pars inferior (except the reinforced area of the saccular wall) and utriculo-canal morphology that minimizes stress proclivity among mammals (Pender 2014b, 2015). The fibrous trabecular meshwork of connective tissue within the perilymphatic space surrounding the membranous labyrinth of the pars superior (Pender 2018) could also buffer against perturbations in the pars inferior. No such meshwork exists around the saccule, DR, or proximal cochlear duct and vestibular caecum. These membranous structures, however, do abut the bone (spherical recess, crista reuniens, and spiral laminae, respectively) and the saccule possesses a reinforced anterolateral wall in *Macaca mulatta* (rhesus macaque), *Saimiri sciureus* (squirrel monkey), flying squirrels (species not reported), and most commonly in *Homo sapiens* (this reinforcement was first described by Perlman 1940; see also Bast and Anson 1949; Igarashi 1964). The membrana limitans, a thin membrane spanning the vestibule, also provides structural support for the pars superior (Hara and Kimura 1993; Mukherjee et al. 2019; Smith et al. 2021). In combination with the features listed above, the DR may contribute to preservation of vestibular function, particularly during cochlear trauma. This is related to three characteristics of the duct: (1) its overall flattened tube-like structure; (2) the small intralumenal diameter of its middle third; and (3) thinner walls in the middle and cochlear thirds relative to the vestibular third potentially reflecting a reduction in stiffness. These three features all contribute to a possible valve-like function of the DR, where the middle third collapses in on itself either in states of low endolymphatic pressure or when the cochlear duct is removed preventing vestibular endolymph loss. These varying states of DR patency have been noted before in sectioned pediatric temporal bones (Bachor and Karmody 1995), in synchrotron phase contrast imaging of adult temporal bones (Li et al. 2021), and in sectioned guinea pig temporal bones during obliteration of the endolymphatic duct (Konishi 1977).

It should be noted that if the DR closes during surgical removal of the cochlea, endolymph production and maintenance in the vestibular labyrinth (e.g., via the dark cell epithelia and subepithelial melanocytes) may prove sufficient to maintain endolymph K^+ levels even in the absence of the stria vascularis of the cochlear duct (for a review of endolymph secretion see Köppl et al. 2018). Some leakage of endolymph is possible in this scenario, although the rate at which this would occur may not affect K^+ levels in the endolymph (as discussed in Plontke et al. 2021).

The incorporation of our new DR morphology metrics into biophysical models of the membranous labyrinth (e.g., Pender, 2009, 2014a, 2019) can test hypotheses regarding the DR's role in vestibular protection during trauma. In combination with thickened pars superior membranes and decreased stress proclivity, the three characteristics of the DR outlined above may constitute a "first barrier" of the membranous vestibular labyrinth against endolymphatic disturbances of cochlear origin. Features of the membranous pars superior would then provide overall protection of the vestibular labyrinth to general physical trauma. Future biophysical modeling of fluid and ductal dynamics, particularly related to DR morphology, will shed further light on these issues.

Role in Ménière's Disease

Ménière's disease is characterized by vertigo and hearing loss (for review see Espinosa-Sanchez and Lopez-Escamez 2016). The central cause is likely a build-up of endolymph (endolymphatic hydrops) within the labyrinth (Hallpike and Cairns 1938; Yamakawa 1938) Recently, it has been hypothesized that the DR plays a role in the development of endolymphatic hydrops during obstruction or permanent closure (for review, see Hornibrook et al. 2021). Our measurements of DR morphology contribute to improved models of the DR's potential role in endolymphatic hydrops. For example, one hypothesis posits that the DR could become blocked by masses of dislodged saccular otoconia (average human utricular otoconia size has been reported to be 0.010 mm, Walther et al. 2014; average saccular otoconia size is not available). The presence of such blockages impeding endolymph flow through the DR is supported by previous work showing displaced saccular otoconia within the DR leading to cochlear hydrops (Kitamura et al. 1982). Incorporating our new DR metrics (particularly DR width and wall thickness) in updated models of cochleo-saccular membrane viscoelastoplasticity (Pender 2019) accounting for membrane displacement (Pender 2018), and fluid pressures during hydrops (Warmerdam et al. 2003) could then be applied to further test hypotheses of the DR's role in endolymphatic hydrops.

The orientation of the DR within the cranium may also affect otoconial blockage. For example, the more superoinferior position of the vestibular third of the DR paired with its curved shape may funnel dislodged otoconia into the narrow and more horizontally oriented middle third. Ultimately, such data on orientation of the DR within the cranium will provide additional variables to incorporate into updated biophysical models of DR function.

The Evolution of the DR and Cochlear Duct

The evolutionary history of the vertebrate inner ear is of intense interest to a variety of fields including comparative biology, paleontology, and human medicine. Indeed, many clinical breakthroughs in otology were made possible through careful examination of comparative inner ear physiology and evolutionary changes in morphology (e.g., Curthoys et al. 1977, 1982; Janesick and Heller 2019; Oshima et al. 2007; for reviews, see Lundberg et al. 2015; Jackler and Jan 2019). Great strides have been made in deciphering morphological changes of the inner ear throughout vertebrate evolution, particularly related to the semicircular canals (e.g., Bronzati et al. 2021; Higuchi et al. 2019; Morimoto et al. 2020; Spoor and Zonneveld 1998; Urciuoli et al. 2020; for a review see Fritzsch et al. 2014) and cochlea (Luo et al. 1995; Luo et al. 2016; for a review see Manley 2012). However, the communication structure between the peripheral auditory and vestibular systems remains enigmatic. This is in part due to the difficulty in visualizing morphological variation of the DR, otolith organs, and cochlear duct in extant species, and observing such variation in bony structure (e.g., when studying fossils).

Detailed descriptions of DR morphology will elucidate the DR's role in differential evolutionary trajectories of the peripheral auditory and vestibular systems. For example, the small dimensions of the DR reported here may serve to maintain the high endolymphatic potential observed among mammalian cochleae. Modern therians (marsupial and placental mammals) exhibit a uniquely high potential in their cochlear endolymph (+80 and +120 mV; Fettiplace 2017; Schmidt and Fernández 1962) relative to the vestibular labyrinth compared to all other vertebrates (Köppl et al. 2018; recent review in Köppl and Manley 2019). This extraordinarily high potential in mammalian cochlear endolymph may be linked with sensitivity to higher frequency hearing, a unique feature of the mammalian lineage (Wilms et al. 2016). One possible reason for this high potential (at least in eutherians) is certain cellular specializations in the stria vascularis which produces endolymph (Köppl et al. 2018; Wilms et al. 2016). Another possibility is that the small dimensions of the DR reported here play a role in maintaining this high endolymphatic potential in the mammalian cochlea. Such a small, flattened ductal connection between vestibular and cochlear labyrinths could inhibit fluid transfer between the two. Examination of DR morphology among other mammalian and non-mammalian taxa will test this hypothesis further.

Our results provide a morphological assessment of the human DR and its association to a specific feature of the bony labyrinth: the CR. The CR (observable in our scans up to 0.110 mm voxel resolution) runs just posterior to where the OSL emerges from the otic capsule wall. The CR serves as a useful feature for comparative anatomists and paleontologists to examine changes in the DR when soft tissue is not present. In addition, the continuity between the CR and OSL raises the possibility that there is both a structural and functional relationship between the two. Future histological work on the development of this region should elucidate the relationship between the two structures and shed light on the CR's potential evolutionary significance.

This study establishes the DR's morphology and 3D spatial configuration to surrounding structures in relation to cranial planes via CR orientation. Our results provide a basis upon which we can begin to build a clearer understanding of the DR's role in inner ear function and disease and identify its place within the evolutionary story of the vertebrate inner ear. These observations shed light on the importance the DR has as being both a functional and evolutionary bridge of the inner ear amongst mammals.

ACKNOWLEDGEMENTS

The authors acknowledge the facilities and the scientific and technical assistance of Microscopy Australia at the Australian Centre for Microscopy & Microanalysis at the University of Sydney. We also thank the Institute of Anatomy and Cell Biology, Martin Luther University Halle-Wittenberg, Halle (Saale), Germany (Director Prof. Dr. med. Heike Kielstein) for providing the temporal bone specimen for Fig. 8. CT scan data of human crania used for Group 2 were provided by Dr. Ashley Hammond and Dr. Sergio Almécija, with the resources and coordination of the American Museum of Natural History's Microscopy and Imaging Facility. In particular, we thank Morgan Chase, Andrew Smith, and Alisha Anaya for assistance during scanning.

Funding This work was supported by an NSF Doctoral Dissertation Research Improvement Grant (award #: 2051335); the Garnett Passe and Rodney Williams Memorial Foundation; the Graduate Center, City University of New York; the Center for Anatomy and Functional Morphology at the Icahn School of Medicine at Mount Sinai; and the New York Consortium in Evolutionary Primatology.

Declarations

Conflict of Interest The authors declare no competing interests.
Outside the submitted work, the following financial activities are declared:
SKP (last 3 years):
Personal Consultancies: AudioCure Pharma GmbH, Berlin, Germany.
Institutional research collaborations: MEDEL, Austria; Cochlear, Australia; Oticon Medical, Denmark; Schwabe Arzneimittel, Germany.
Travel support for lectures: MED-EL, Austria.
Honorary for Lectures or Session Moderations: Infectopharm, Germany; Merck Serono, Darmstadt, Germany; Schwabe Arzneimittel, Germany

REFERENCES

3D Slicer (2020) 3D Slicer. [Software]. Retrieved from https://www.slicer.org

Anniko M, Lundquist P (1977) The influence of different fixatives and osmolality on the ultrastructure of the cochlear neuroepithellum*. Arch Otorhinolaryngol 218:67–78

Bachor E, Karmody C (1995) The utriculo-endolymphatic valve in pediatric temporal bones. Eur Arch Otorhinolaryngol 252(3):167–171

Bast TH, Anson BJ (1949) The temporal bone and the ear. Thomas, C.C

Bronzati M, Benson RBJ, Evers SW, Witmer LM, Langer MC, Nesbitt SJ (2021) Deep evolutionary diversification of semicircular canals in archosaurs. Curr Biol. https://doi.org/10.1016/j.cub.2021.03.086

Curthoys I, Blanks R, Markham C (1982) Semicircular canal structure during postnatal development in cat and guinea pig. Annals of Otology, Rhinology and Laryngology 91(2):185–192

Curthoys IS, Markham CH, Curthoys EJ (1977) Semicircular duct and ampulla dimensions in cat, guinea pig and man. J Morphol 151(1):17–34. https://doi.org/10.1002/jmor.1051510103

Espinosa-Sanchez JM, Lopez-Escamez JA (2016) Menière's disease. In Handbook of Clinical Neurology (Vol. 137, pp. 257–277). Elsevier B.V. https://doi.org/10.1016/B978-0-444-63437-5.00019-4

Fedorov A, Beichel R, Kalpathy-Cramer J, Finet J, Fillion- Robin J-C, Pujol S, Kikinis R (2012) 3D slicer as an image computing platform for the quantitative imaging network. Magn Reson Imaging 30(9):1323–1341

Fettiplace R (2017) Hair cell transduction, tuning, and synaptic transmission in the mammalian cochlea. Compr Physiol 7(4):1197–1227. https://doi.org/10.1002/cphy.c160049

Fritzsch B, Kopecky BJ, Duncan JS (2014) Development of the mammalian "vestibular" system: evolution of form to detect angular and gravity acceleration. In Development of Auditory and Vestibular Systems: Fourth Edition (pp. 339–367). Elsevier Inc. https://doi.org/10.1016/B978-0-12-408088-1.00012-9

Hallpike CS, Cairns H (1938) Observations on the pathology of Menicre's syndrome. In Proceedings of the Royal Society of Medicine (Vol. 31, Issue Sept., pp. 55–74)

Hara M, Kimura RS (1993) Morphology of the membrana limitans. Annals of Otology, Rhinology & Laryngology 102(8):625–630. https://doi.org/10.1177/000348949310200811

Higuchi S, Sugahara F, Pascual-Anaya J, Takagi W, Oisi Y, Kuratani S (2019) Inner ear development in cyclostomes and evolution of the vertebrate semicircular canals. Nature 565(7739):347–350. https://doi.org/10.1038/s41586-018-0782-y

Hornibrook J, Mudry A, Curthoys I, Smith CM (2021) Ductus reuniens and its possible role in Menière's disease. Otol Neurotol 42(10):1585–1593. https://doi.org/10.1097/MAO.0000000000003352

Igarashi M (1964) Comparative histological study of the reinforced area of the saccular membrane in mammals. Research Report. Naval School of Aviation Medicine (U.S.), 1–14

Jackler RK, Jan TA (2019) The future of otology. J Laryngol Otol 133(9):747–758. https://doi.org/10.1017/S0022215119001531

Janesick AS, Heller S (2019) Stem cells and the bird cochlea—where is everybody? Cold Spring Harb Perspect Med 9(4):a033183. https://doi.org/10.1101/cshperspect.a033183

Kikinis R, Pieper SD, Vosburgh K (2014) 3D slicer: a platform for subject-specific image analysis, visualization, and clinical support. Intraoperative Imaging Image-Guided Therapy 3(19):277–289

Kitamura K, Schuknecht HF, Kimura RS (1982) Cochlear hydrops in association with collapsed saccule and ductus reuniens. Ann Otol 91:5–13

Konishi S (1977) The ductus reuniens and utriculo-endolymphatic valve in the presence of endolymphatic hydrops in guinea-pigs. J Laryngol Otol 91(12):1033–1045

Köppl C, Manley GA (2019) A functional perspective on the evolution of the cochlea. Cold Spring Harbor Perspectives in Medicine 9(6). https://doi.org/10.1101/cshperspect.a033241

Köppl C, Wilms V, Russell IJ, Nothwang HG (2018) Evolution of endolymph secretion and endolymphatic potential generation in the vertebrate inner ear. Brain Behav Evol 92(1):1–31. https://doi.org/10.1159/000494050

Li H, Rajan GP, Shaw J, Rohani SA, Ladak HM, Agrawal S, Rask-Andersen H (2021a) A synchrotron and micro-ct study of the human endolymphatic duct system: is Meniere's disease caused by an acute endolymph backflow? Front Surg 8(662530). https://doi.org/10.3389/fsurg.2021.662530

Li H, Schart-Moren N, Rajan G, Shaw J, Rohani SA, Atturo F, Ladak HM, Rask-Andersen H, Agrawal S (2021b) Vestibular organ and cochlear implantation–a synchrotron and micro-CT study. Frontiers in Neurology 12(663722). https://doi.org/10.3389/fneur.2021.663722

Lundberg YW, Xu Y, Thiessen KD, Kramer KL (2015) Mechanisms of otoconia and otolith development. Dev Dyn 244:239–253. https://doi.org/10.1002/dvdy

Luo Z-X, Crompton AW, Lucas SG (1995) Evolutionary origins of the mammalian promontorium and cochlea. J Vertebr Paleontol 15(1):113–121. https://doi.org/10.1080/02724634.1995.10011211

Luo Z-X, Schultz JA, Ekdale EG (2016) Evolution of the middle and inner ears of mammaliaforms: the approach to mammals. In Evolution of the Vertebrate Ear (pp. 139–174). https://doi.org/10.1007/978-3-319-46661-3_6

Manley GA (2012) Evolutionary paths to mammalian cochleae. J Assoc Res Otolaryngol 13(6):733–743. https://doi.org/10.1007/s10162-012-0349-9

Morimoto N, Kunimatsu Y, Nakatsukasa M, Ponce de León MS, Zollikofer CPE, Ishida H, Sasaki T, Suwa G (2020) Variation of bony labyrinthine morphology in Mio−Plio−Pleistocene and modern anthropoids. Am J Phys Anthropol 173(2):276–292. https://doi.org/10.1002/ajpa.24098

Mukherjee P, Cheng K, Curthoys I (2019) Three-dimensional study of vestibular anatomy as it relates to the stapes footplate and its clinical implications: an augmented reality development. J Laryngol Otol 133(3):187–191. https://doi.org/10.1017/S0022215119000239

Oshima K, Grimm CM, Corrales CE, Senn P, Martinez Monedero R, Géléoc GSG, Edge A, Holt JR, Heller S (2007) Differential distribution of stem cells in the auditory and vestibular organs of the inner ear. J Assoc Res Otolaryngol 8(1):18–31. https://doi.org/10.1007/s10162-006-0058-3

Pender DJ (2009) A model analysis of static stress in the vestibular membranes. Theoretical Biology and Medical Modelling 6(1). https://doi.org/10.1186/1742-4682-6-19

Pender DJ (2014a) A model design for the labyrinthine membranes in mammals. Laryngoscope 124(6):E245–E249. https://doi.org/10.1002/lary.24516

Pender DJ (2014b) Membrane stress proclivities in the mammalian labyrinth. International Archives of Otorhinolaryngology 18(4):398–402. https://doi.org/10.1055/s-0034-1385846

Pender DJ (2015) Membrane stress in the human labyrinth and Meniere disease: a model analysis. International Archives of Otorhinolaryngology 19(4):336–342. https://doi.org/10.1055/s-0035-1549157

Pender DJ (2018) Suspensory tethers and critical point membrane displacement in endolymphatic hydrops. International Archives of Otorhinolaryngology 22(3):214–219. https://doi.org/10.1055/s-0037-1604474

Pender DJ (2019) A model of viscoelastoplasticity in the cochleosaccular membranes. Laryngoscope Investigative Otolaryngology 4(6):659–662. https://doi.org/10.1002/lio2.318

Perlman H (1940) The saccule: observations on a differentiated reinforced area of the saccular wall in man. Arch Otolaryng 32:678–691

Pixologic (2020) Zbrush. [Software]. Version 4R8. Retrieved from https://pixologic.com

Plontke SK, Rahne T, Curthoys IS, Håkansson B, Fröhlich L (2021) A case series shows independent vestibular labyrinthine function after major surgical trauma to the human cochlea. Commun Med1(1). https://doi.org/10.1038/s43856-021-00036-w

Schmidt RS, Fernández Cés (1962) Labyrinthine DC potentials in representative vertebrates. J Cell Comp Phys 59(3):311–322. https://doi.org/10.1002/jcp.1030590311

Smith CM, Curthoys IS, Mukherjee P, Wong C, Laitman JT (2021) Three-dimensional visualization of the human membranous labyrinth: the membrana limitans and its role in vestibular form. The Anatomical Record, ar.24675. https://doi.org/10.1002/ar.24675

Spoor F, Zonneveld F (1998) Comparative review of the human bony labyrinth. American Journal of Physical Anthropology, Suppl 27:211–251. https://doi.org/10.1002/(SICI)1096-8644(1998)107:27+%3c211::AID-AJPA8%3e3.0.CO;2-V

Urciuoli A, Zanolli C, Beaudet A, Dumoncel J, Santos F, Moyà-Solà S, Alba DM (2020) The evolution of the vestibular apparatus in apes and humans. Elife 9:1–33. https://doi.org/10.7554/eLife.51261

Uzun H, Curthoys IS, Jones AS (2007) A new approach to visualizing the membranous structures of the inner ear - High resolution X-ray micro-tomography. Acta Otolaryngol 127(6):568–573. https://doi.org/10.1080/00016480600951509

Uzun-Coruhlu H, Curthoys IS, Jones AS (2007) Attachment of the utricular and saccular maculae to the temporal bone. Hear Res 233(1–2):77–85. https://doi.org/10.1016/j.heares.2007.07.008

Walther LE, Wenzel A, Buder J, Blocking MB, Kniep R, Blödow A (2014) Detection of human utricular otoconia degeneration in vital specimen and implications for benign paroxysmal positional vertigo. Eur Arch Otorhinolaryngol 271(12):3133–3138. https://doi.org/10.1007/s00405-013-2784-6

Warmerdam TJ, Schröder FHHJ, Wit HP, Albers FWJ (2003) Perilymphatic and endolymphatic pressures during endolymphatic hydrops. Eur Arch Otorhinolaryngol 260(1):9–11. https://doi.org/10.1007/s00405-002-0518-2

Wilms V, Köppl C, Söffgen C, Hartmann AM, Nothwang HG (2016) Molecular bases of K + secretory cells in the inner ear: shared and distinct features between birds and mammals Sci Rep 6. https://doi.org/10.1038/srep34203

Yamakawa K (1938) Uber die pathologisch Veranderung bei einem Ménière-Kranken. J Otorhinolaryngol Soc Jpn 4:2310–2312

Yamane H, Takayama M, Sunami K, Sakamoto H, Mochizuki K, Inoue Y (2009) Three-dimensional images of the reuniting duct using cone beam CT. Acta Otolaryngol 129(5):493–496. https://doi.org/10.1080/00016480802294393